

# Thermooxidative Decomposition and Its Kinetics on Chlorinated Natural Rubber from Latex

JIE-PING ZHONG,<sup>1</sup> SI-DONG LI,<sup>1</sup> HE-PING YU,<sup>1</sup> YONG-CAI WEI,<sup>1</sup> ZHENG PENG,<sup>1</sup> JU-LAN QU,<sup>2</sup> CHEN-KUN GUO<sup>2</sup>

<sup>1</sup> South China Tropical Agricultural Product Processing Research Institute, P.O. Box 318, Zhanjiang 524001, People's Republic of China

<sup>2</sup> Test Center, Zhanjiang Normal College, Zhanjiang 524048, People's Republic of China

Received 6 July 1999; accepted 25 February 2000

**ABSTRACT:** Thermooxidative decomposition and its kinetics on chlorinated natural rubber (CNR) from latex are studied by thermal gravimetry (TG) analysis and TG coupled with FTIR spectroscopy. The thermooxidative decomposition of CNR is a two-step reaction. The first step is the reaction of dehydrochlorination of which the reaction order ( $n$ ) is 1.1; the reaction activation energy ( $E$ ) increases linearly with the increment of the heating rate ( $B$ ), and the apparent activation energy ( $E_0$ ) is 101.7 kJ/mol. The initial temperature of weight loss ( $T_0$ ) is  $1.29B + 248.7$ , the final temperature of weight loss ( $T_f$ ) is  $0.86B + 312.4$ , and the temperature at the maximum weight loss ratio ( $T_p$ ) is  $1.05B + 286.2$ . The decomposition ratio at  $T_p$  ( $C_p$ ) is not affected by  $B$ , and its average value is 38%. The decomposition ratio at  $T_f$  ( $C_f$ ) is also not affected by  $B$ , and its average value is 60%. The second step is an oxidative decomposition reaction of the molecular main chain. The value of  $n$  is 1.1,  $E$  increases linearly with the increment of  $B$ ,  $E_0$  is 125.0 kJ/mol, the relation between  $B$  and  $T$  is similar to that of the first step, and  $C_f$  approaches 100%. © 2001 John Wiley & Sons, Inc. *J Appl Polym Sci* 81: 1305–1309, 2001

**Key words:** latex; chlorinated natural rubber; thermooxidative decomposition; kinetics

## INTRODUCTION

Chlorinated natural rubber (CNR), which is prepared by the chlorinated modification of NR from solution or latex,<sup>1</sup> has such properties as good film formation, acid proof, alkali proof, corrosion resistance, antipenetrability, inflammation resistance, and thermal stability. It has been applied in the production of raw materials for paints and adhesives, as an additive for ink, and in acid-proof and alkali-proof products. The traditional  $\text{CCl}_4$  solution process has been prohibited in many coun-

tries because it has disadvantages such as high equipment investment, being environmentally polluting, and being harmful to the health of workers. This makes the production of CNR from latex have a vast vista. Two groups<sup>2,3</sup> studied the preparation of CNR. Another<sup>4,5</sup> studied the molecular structure of CNR by H-NMR and C-NMR methods. The chlorination mechanism of CNR was studied in detail,<sup>6–8</sup> but up to now there have been few reports on the thermooxidative decomposition of CNR. This article reports the thermal decomposition kinetics of CNR from latex in air at different heating rates ( $B$ ) by the use of thermal gravimetry (TG) analysis and FTIR/TG coupling system. The compositions of gases evolved during the thermooxidative decomposition of CNR were identified. The reaction order ( $n$ ), the activation en-

Correspondence to: S.-D. Li.  
Contract grant sponsor: Chinese Natural Science Foundation.

*Journal of Applied Polymer Science*, Vol. 81, 1305–1309 (2001)  
© 2001 John Wiley & Sons, Inc.

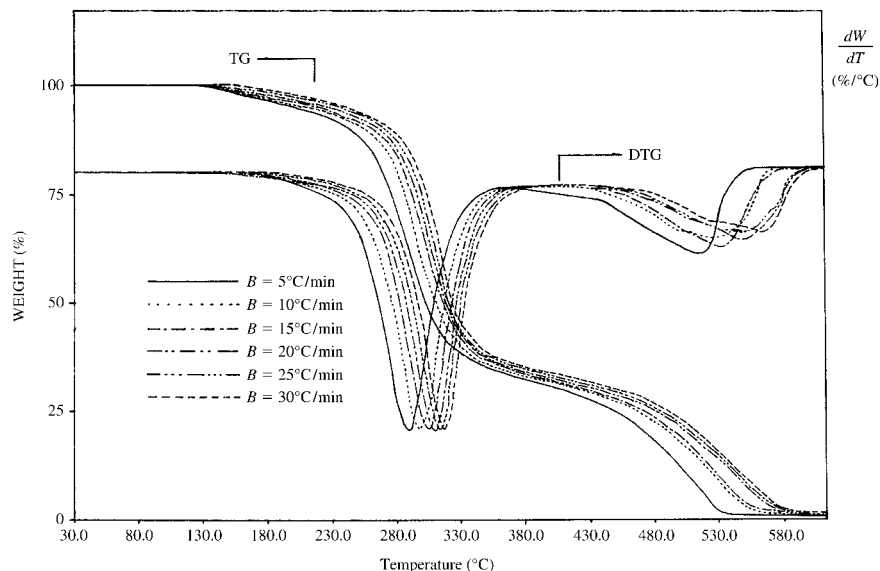


**Figure 1** The TG and DTG curves of thermooxidative decompositions of CNR.

ergy ( $E$ ), and the frequency factor ( $A$ ) with a maximum correlated coefficient ( $r$ ) were calculated. The apparent activation energy ( $E_0$ ) was obtained by linear regression, and the relation between  $B$  and the decomposition temperature  $T$  and the decomposition ratio  $C$  were also discussed.

## EXPERIMENTAL

### Materials

A certain amount of distilled water was added into a three-necked, round-bottomed flask. The

temperature was kept constant with a water bath, and chlorine gas was passed into the water to saturation. The NR latex stabilized with Vulcanstab LW was added while stirring. At the same time the chlorine gas was passed into the flask continuously. A CNR with preliminary chlorination was produced. We kept passing the chlorine gas into the flask to the predetermined reaction time and then stopped the reaction. The product was neutralized with a diluted sodium hydroxide solution to make the pH of the reaction system 7–8. The product was filtered and washed with distilled water and then dried in a vacuum at 50°C to get the powder CNR sample.

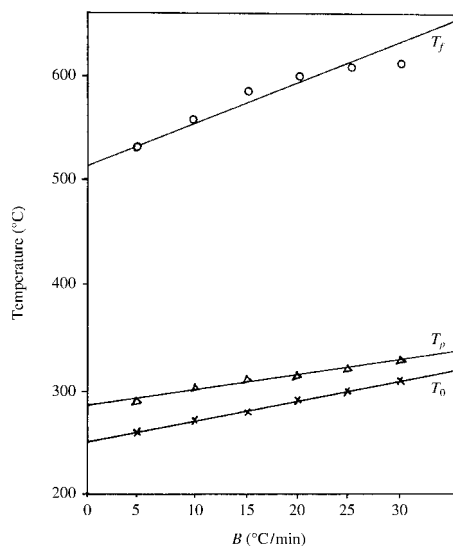


**Figure 2** The relation between  $B$  and  $T$  in the first-step reaction.

### TG and FTIR/TG Analysis

The TG analysis was carried out using a Perkin Elmer TG S-2 thermal gravimetric analyzer. The mass of the sample was 8.00 mg. The carrier gas was air, and its flow rate was 50 mL min<sup>-1</sup>. The temperature rose from 30 to 600°C at a heating rate of 5, 10, 15, 20, 25, and 30°C min<sup>-1</sup>, respectively.

The FTIR/TG analysis was carried out using a DuPont-2100 thermal gravimetric analyzer coupled with a Nicolet-550 FTIR spectrometer. The FTIR spectra were recorded in a wave number range of 4000–400 cm<sup>-1</sup> with a spectral resolution of 4 cm<sup>-1</sup> and a scanning frequency of 20. The mass of the sample was 8.00 mg. The carrier gas was air, and its flow rate was 50 mL min<sup>-1</sup>. The temperature rose from 30 to 600°C.

**Table I** Relation between  $B$  and  $C$  in First-Step Reaction

	$B$ ( $^{\circ}\text{C min}^{-1}$ )						Average
	5	10	15	20	25	30	
$C_p$ (%)	39	39	37	38	38	39	38
$C_f$ (%)	61	60	60	60	60	60	60

### Data Processing

The reaction kinetic factors were obtained by the processing of TG data through the Coats–Redfern integral method.<sup>9</sup> From the mathematic processing of the reaction kinetic equation  $d\alpha/dt = k(1 - \alpha)^n$  and the Arrhenius equation  $K = Ae^{-E/RT}$ , the following equation can be obtained:

$$\ln\{[1 - (1 - \alpha)^{1-n}]/[T^2(1 - n)]\} = \ln[(1 - 2RT/E)AR/BE] - E/RT \quad (n \neq 1)$$

in which  $n$  is the reaction order,  $\alpha$  is the reaction degree,  $T$  is the absolute temperature,  $B$  is the heating rate,  $E$  is the reaction activation energy,  $R$  is the gas constant, and  $A$  is the frequency factor. When  $n \neq 1$ , a line can be obtained from the plot of  $\ln\{[1 - (1 - \alpha)^{1-n}]/[T^2(1 - n)]\}$  versus  $1/T$ , of which the slope is  $-E/R$ , and the intercept is  $\ln[(1 - 2RT/E)AR/BE]$ . Adopting the least squares fitting method with different  $n$ , the  $n$  of the maximum correlated coefficient ( $r$ ) is the calculated reaction order, and the corresponding  $E$  is the expected activation energy.

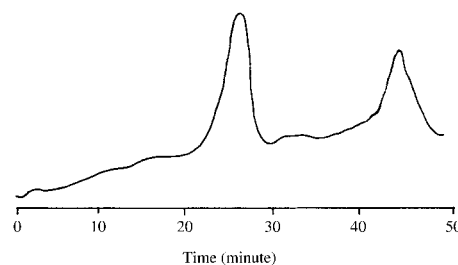
## RESULTS AND DISCUSSIONS

### Effect of Heating Rate on Process of Thermal Decomposition

The thermooxidative decomposition of CNR was carried out in air. Figure 1 depicts the TG and DTG curves of thermooxidative decompositions of CNR at six different heating rates. There are two obvious

**Table II** Relation between  $B$  and  $C$  in Second-Step Reaction

	$B$ ( $^{\circ}\text{C min}^{-1}$ )						Average
	5	10	15	20	25	30	
$C_f$ (%)	99	100	100	100	100	100	100

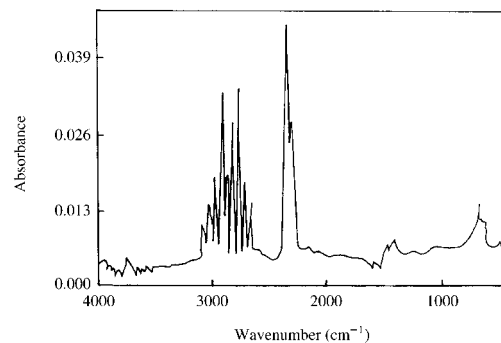
**Figure 3** The Gram–Schmidt curve for CNR.

turns on the TG curves and two corresponding peaks on the DTG curves, indicating that the thermooxidative decomposition of CNR could be a two-step reaction. The first weight loss peak at 160–390 $^{\circ}\text{C}$  might be assigned to the dehydrochlorination reaction. The second weight loss peak at 390–585 $^{\circ}\text{C}$  might be assigned to the second step of the thermal decomposition. The TG and DTG curves shift toward the high temperature with the increment of heating rate. The reactions at six different heating rates are similar to each other.

### Relation between Heating Rate and Temperature

Figure 2 shows the relations between  $B$  and the decomposition temperature ( $T$ ). The TG curves are obtained from the initial temperature of weight loss ( $T_0$ ) and the final temperature of weight loss ( $T_f$ ) and  $T_p$  is the temperature of the maximum weight loss rate. The width of the weight loss peak can be expressed as  $T_f - T_0$ . It can be seen from Figure 2 that the thermal decomposition temperatures increase along with the increment of  $B$ , indicating that the  $B$  has a significant effect on  $T$ . The relations between  $B$  and  $T$  are as follows:

$$T_0 = 1.29B + 248.7$$

**Figure 4** IR spectra of gases evolved in the first step of thermooxidative decomposition.

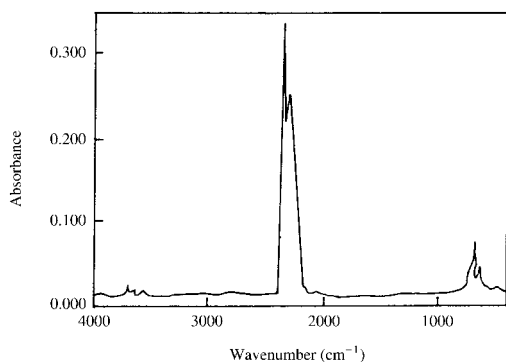


**Figure 5** IR spectra of gases evolved in the second step of thermooxidative decomposition.

$$T_p = 1.05B + 286.2$$

$$T_f = 0.86B + 312.4$$

Because the thermooxidative temperature linear increase with the increment of  $B$  is caused by the heat hysteresis, the thermooxidative temperatures should be expressed more exactly in equilibrium temperatures (which are the decomposition temperatures when  $B$  approaches zero) with the elimination of heat hysteresis. The equilibrium decomposition temperatures of CNR are expressed as follows:

$$T_0^0 = 248.7$$

$$T_p^0 = 286.2$$

$$T_f^0 = 312.4$$

The width of the peak is expressed as  $T_f - T_0 = -0.43B + 63.7$ , and it decreases with the increment of  $B$ . The relation between  $B$  and  $T$  in the second-step reaction is similar to that of the first step.

#### Effect of Heating Rate on Thermooxidative Decomposition Rate

Table I shows the relationship between  $B$  and  $C$  in the first-step reaction. The  $C_p$  and  $C_f$  are the

thermooxidative decomposition ratios at  $T_p$  and  $T_f$ , respectively:

$$C_p = 100\% - \text{wt \% of residues}$$

$$C_f = 100\% - \text{wt \% of residues}$$

The results indicate that  $C_p$  and  $C_f$  are not affected by  $B$ , and their mean values are 38 and 60%, respectively.

Table II shows the relationship between  $B$  and  $C_f$  in the second-step reaction. The  $C_f$  is not affected by  $B$  and approaches 100%, indicating that the second thermooxidative decomposition proceeds thoroughly.

#### Identification of Evolved Gases during Thermooxidative Decomposition

The Gram-Schmidt curve of the evolved gases during the thermooxidative decomposition can be obtained by the Gram-Schmidt orthodoxy vector method (see Fig. 3). The peak at 27.27–28.31 min on the Gram-Schmidt curve corresponds to the gases evolved in the first-step reaction. The peak at 46.54–51.43 min corresponds to the gases evolved in the second-step reaction.

Figure 4 depicts the IR spectra of the evolved gas at 27.27–28.31 min in the first-step reaction. By comparing them with the standard spectra, the main product is found to be HCl with a little  $\text{CO}_2$ , indicating that HCl is eliminated from CNR by the scission of C—Cl and C—H bonds at 160–390°C. At the same time, a little oxidative reaction occurs on the main chain.

Figure 5 depicts the IR spectra of the evolved gas at 46.54–51.43 min in the second-step reaction. The corresponding product is only  $\text{CO}_2$ , which is caused by the oxidative scission of the main chain of the CNR.

#### Kinetics of Thermooxidative Decomposition

Table III shows the kinetic parameters in the first-step reaction. It can be seen that the mean

**Table III** Reaction Orders and Activation Energies of First-Step Reaction

	$B$ ( $^{\circ}\text{C min}^{-1}$ )					
	5	10	15	20	25	30
$n$	1.1	1.1	1.0	1.1	1.1	1.2
$E$ ( $\text{kJ mol}^{-1}$ )	105.3	109.9	115.0	120.0	124.1	125.8
$A \times 10^{-10}$	0.10	0.38	1.39	3.89	10.72	16.21
$r$	0.997	0.996	0.995	0.995	0.995	0.995

**Table IV** Reaction Orders and Activation Energies of Second-Step Reaction

	$B$ ( $^{\circ}\text{C min}^{-1}$ )					
	5	10	15	20	25	30
$n$	1.1	1.1	1.0	1.1	1.1	1.2
$E$ ( $\text{kJ mol}^{-1}$ )	144.6	163.9	172.2	180.1	203.6	205.7
$A \times 10^{-11}$	0.01	0.22	1.23	3.06	135.70	183.10
$r$	0.995	0.997	0.997	0.996	0.995	0.995

value of  $n$  at different  $B$  is 1.1, indicating that the dehydrochlorination is a reaction with the order of 1.1. The  $E$  increases linearly with the increment of  $B$ . From the linear regression adopting the least squares method, the calculated apparent activation energy  $E_0$  at a  $B$  of  $0^{\circ}\text{C min}^{-1}$  is  $101.7 \text{ kJ mol}^{-1}$ , which is close to the effective activation energy of the dehydrochlorination reaction of poly(vinylchloride) (PVC,  $94\text{--}126 \text{ kJ mol}^{-1}$ ).<sup>9</sup> The  $A$  is in direct proportion with  $B$ . The values of the correlated coefficient ( $r$ ) are over 0.995.

Table IV shows the kinetic parameters in the second-step reaction. It can be seen that  $n$  is not affected by  $B$  and the mean value of  $n$  at different  $B$  is 1.1. The value of  $E$  increases linearly with an increment of  $B$ . The calculated  $E_0$  is  $125.0 \text{ kJ mol}^{-1}$ . The  $A$  increases rapidly with  $B$ . The values of  $r$  are over 0.995.

The thermooxidative decomposition reaction of CNR takes place in hot air because of the existence of  $\text{O}_2$ . The first-step reaction occurs at  $160\text{--}390^{\circ}\text{C}$  and is mainly the dehydrochlorination from the main chain. The activation energy is close to that of the dehydrochlorination of PVC. The second-step reaction occurs at  $390\text{--}585^{\circ}\text{C}$  and is the oxidative decomposition of the main chain.

## CONCLUSION

The thermooxidative decomposition of CNR is a two-step reaction. At the first-step reaction, the

thermal decomposition temperatures increases linearly with the increment of  $B$ . The equilibrium temperatures are  $T_0^0 = 248.7$ ,  $T_p^0 = 286.2$ , and  $T_f^0 = 312.4$ . The width of the peak on the DTG curve decreases linearly with the increment of  $B$ . The  $C_p$  and  $C_f$  are not affected by  $B$ , and the mean values are 38 and 60%, respectively. At the second-step reaction, the effects of  $B$  on  $T$  and  $C$  are similar to that of the first-step reaction.

The first step of the thermooxidative decomposition of CNR is a reaction of dehydrochlorination, and the second one is the oxidative scission of the main chain. The reaction orders of the two steps are 1.1, and  $E$  increases linearly with the increment of  $B$ . The apparent activation energies of the two steps are  $101.7$  and  $125.0 \text{ kJ mol}^{-1}$ , respectively.

## REFERENCES

- Huang, Y.-X. Guangzhou Chem Ind 1989, 2, 8.
- Li, S.-D. et al. Chin Rubber Ind 1998, 8, 497.
- Blood, G. F. Rubber Chem Technol 1934, 7, 320.
- Eskina, M. V. Eur Polym J 1990, 26, 181.
- Eskina, M. V. Vysokomol Soedin Ser A 1988, 30, 142.
- Van Amerogen, G. J. Rubber Chem Technol 1953, 26, 411.
- Konigsbergen, G. J. Rubber Chem Technol 1953, 26, 406.
- Gerard, K. Rubber Chem Technol 1951, 24, 970.
- Zhao, Q.-X. Chin PVC 1987, 5, 24.